

Crystal-field splitting and the on-site Coulomb energy of $\text{La}_x\text{Sr}_{1-x}\text{TiO}_3$ from resonant soft-x-ray emission spectroscopy

T. Higuchi and T. Tsukamoto

Department of Applied Physics, Science University of Tokyo, Tokyo 162-0825, Japan

M. Watanabe

Photon Factory, KEK, Tsukuba 305-0801, Japan

M. M. Grush and T. A. Callcott

University of Tennessee, Knoxville, Tennessee 37996

R. C. Perera

Advanced Light Source, Lawrence Berkeley Laboratory, Berkeley, California 94720

D. L. Ederer

Physics Department, Tulane University, New Orleans, Louisiana 70118

Y. Tokura

Department of Applied Physics, University of Tokyo, Tokyo 113-8656, Japan

Y. Harada, Y. Tezuka, and S. Shin

Institute for Solid State Physics, University of Tokyo, Tokyo 106-8666, Japan

(Received 8 January 1999; revised manuscript received 17 March 1999)

Resonant soft-x-ray emission spectroscopy was measured on $\text{La}_x\text{Sr}_{1-x}\text{TiO}_3$ ($x=0, 0.05, 0.10$) in the Ti 2*p* energy region. At the Raman scattering of the e_g resonance, the $d-d$ transition whose Raman shift has an energy value of about 2.3 eV corresponds to the crystal-field splitting. On the other hand, at the t_{2g} resonance, the $d-d$ transition whose Raman shift is about 2.2 eV is thought to be the transition reflecting half intra-atomic Coulomb energy. [S0163-1829(99)01232-1]

The Perovskite-type Ti compound SrTiO_3 , which normally has a d^0 configuration,¹ has been extensively studied because a metal-insulator ($M-I$) transition occurs with the substitution of a carrier such as La.²⁻⁴ This system varies from a band insulator with a d^0 configuration to a Mott insulator with a d^1 configuration. The $M-I$ transition is believed to be controlled by the relative magnitudes of the on-site Coulomb energy U and the one electron bandwidth W ; the system is metallic when $U/W < 1$ and is an insulator when $U/W > 1$. Recently, the electronic property of this material has been investigated extensively by Tokura and co-workers.⁵⁻⁸ The apparent plasma frequency increases with increasing La doping, supporting the simple picture of rigid band filling.⁹ Moreover, this fact is supported by an *ab initio* band calculation of Shanthi *et al.*¹⁰ The effective mass deduced from the Drude model increases with increasing La doping for the large doping region ($x > 0.5$) in $\text{La}_x\text{Sr}_{1-x}\text{TiO}_3$, while the effective mass is a constant in lightly doped ($x < 0.5$) in $\text{La}_x\text{Sr}_{1-x}\text{TiO}_3$.^{8,9} Additionally, a similar behavior is also deduced from the electric specific heat coefficient.⁹ These facts indicate that the electron correlation is important when $x > 0.5$, while it is not so important when $x < 0.5$. On the other hand, photoemission spectra have two features in the band gap below the Fermi level (E_F) that correspond to the coherent part at E_F and to the incoherent

part at binding energy of ~ 1.5 eV.¹¹ The relative intensity of these features strongly depends on La doping.

Recently, soft x-ray emission studies (SXES) have been extensively carried out for several 3*d* transition metal compounds, such as TiO_2 ,^{12,13} FeTiO_3 ,¹⁴ SrVO_3 ,¹⁵ and MnO .¹⁶ The soft x-ray emission spectroscopy spectra reflect the electronic structure of the bulk compared with photoelectron spectra, because the mean free path of a soft x ray is very long compared with that of the electron. The Raman scattering observed in the SXES spectra provides useful information about the electronic structure. It is reported that the Raman scattering for these compounds is attributed primary to the $d-d$ transition between the 3*d* valence and conduction bands as well as a charge transfer (CT) transition from an occupied O 2*p* band to unoccupied metal 3*d* band. Compounds that nominally have d^0 configuration as well as compounds with f^0 configuration such as CeO_2 and UO_3 exhibit Raman scattering that is dominantly the CT transition,¹⁷ though they are thought to be a kind of strongly correlated materials.

In this paper, we present soft x-ray emission spectra and soft x-ray absorption spectra (XAS) of $\text{La}_x\text{Sr}_{1-x}\text{TiO}_3$. As a reference, we use the SXES spectra of pure SrTiO_3 .¹⁸ The purpose of this SXES study is to determine experimentally the magnitude of the on-site Coulomb energy and the crystal-field splitting of $\text{La}_x\text{Sr}_{1-x}\text{TiO}_3$ through the study of $d-d$ and CT transitions.

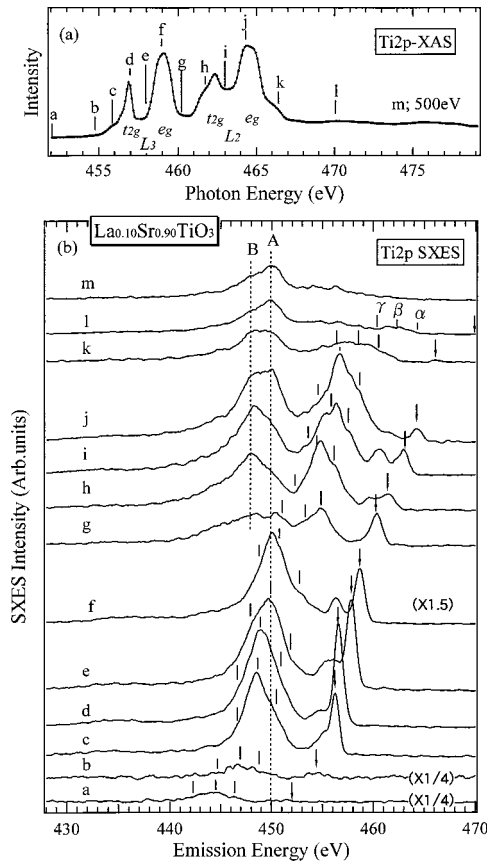


FIG. 1. (a) $Ti\ 2p$ XAS spectra of $Sr_{0.90}La_{0.10}TiO_3$. The numbers indicate the photon energies, where the $Ti\ 2p$ SXES spectra were obtained using photons from beam line 8.0 at the Advanced Light Source (ALS). A Rowland-circle SXF spectrometer with spherical gratings and a photon-counting area detector was used to obtain the SXES spectra.¹⁹ The resolution of the spectrometer was about 0.5 eV at $h\nu=390$ eV. The calibration scale of the spectrometer was determined by measuring the $Ti\ 2p$ XAS and SXES spectra of Ti metal.

Figure 1(a) shows the $Ti\ 2p$ XAS spectrum of $Sr_{0.90}La_{0.10}TiO_3$. The spectrum is derived from two parts of $L_3(2p_{3/2})$ and $L_2(2p_{1/2})$. Furthermore, they are split into t_{2g} and e_g states by the octahedral ligand field.²⁰ Two structures around 471 and 476 eV are the charge-transfer (CT) satellites²¹ corresponding to L_3 and L_2 . It has been reported that the t_{2g} peak decreases with increasing La doping, indicating that the doped electrons enter into the bottom of unoccupied $Ti\ 3d$ band.²² Here, note that the energy position does not depend much on the La doping.²³ The vertical bars, which are labeled from a–m, indicate the selected photon energies for resonant SXES measurements.

Figure 1(b) shows the $Ti\ 2p$ SXES spectra of $Sr_{0.90}La_{0.10}TiO_3$. The $Ti\ 2p$ emission reflects the $Ti\ 3d$ partial density of states. An arrow shown in each spectrum indicates the excitation photon energy. The peak beneath the arrow is attributed to elastic scattering of the excitation photon. The elastic peak is enhanced at the excitation energy corresponding to the t_{2g} absorption peak of L_3 . Then, the peak intensity decreases with increasing of the excitation energy, and is again enhanced slightly at the excitation energies g–j in the region of L_2 absorption shown in Fig. 1(a). This behavior resembles that of TiO_2 (Refs. 12 and 13) and $FeTiO_3$.¹⁴

The spectrum *m* excited at $h\nu=500$ eV is an off-resonance spectrum attributed to the normal $Ti\ 3d \rightarrow Ti\ 2p$ fluorescence spectrum. This spectrum provides evidence indicates that the $Ti\ 3d$ state hybridizes with the $O\ 2p$ state in the valence band. Two dashed lines (A and B peaks) show the fluorescence bands. The A peak corresponds to the bonding state of the valence band. The nonbonding state is expected at around 452–455 eV photon energy. However, the existence of the nonbonding state is not seen clearly in the SXES spectra of Fig. 1. The B peak may be due to the contribution of a satellitelike structure, although the origin is not clear.

Three features shown with vertical bars α , β , and γ represent the energy positions that have energy separation of 5.5, 6.8, and 9.2 eV, respectively, from the excitation energy. They shift as the excitation energy is varied. These features are attributed to the Raman scattering, that is, inelastic scattering. The inelastic scattering that is excited in the L_3 absorption spectral region overlaps with the $Ti\ 3d \rightarrow Ti\ 2p$ fluorescence. The SXES spectra *a* and *b*, excited just below the $Ti\ 2p$ threshold, show a broad peak at a lower energy than the elastic scattering. The fluorescence to the $Ti\ 2p$ core hole can not be observed, because the excitation energy is less than the binding energy of the $Ti\ 2p$ core level. It is attributed to a normal Raman scattering, where the intermediate state of this scattering is a virtual state.

Figure 2 shows the SXES spectra of $La_{0.10}Sr_{0.90}TiO_3$, where the abscissa is the Raman shift that is the energy shift from the elastic scattering. The elastic scattering peak is located at 0 eV. The $Ti\ 3d \rightarrow Ti\ 2p$ fluorescence peaks shown by two vertical bars shift to the higher energy as the excitation energy increases. In $FeTiO_3$, it is reported that the structures appearing in the energy region between 11 and 4 eV can be attributed to the transition to nonbonding $3d^1L$ states and the split-off antibonding satellite is located at 14.5 eV.¹⁵ However, such a satellite is not observed in this figure.

It is known that the elementary excitation of the Raman scattering is the valence band transition. Thus, the Raman scattering can be compared with the optical conductivity spectrum. The optical conductivity spectrum at room temperature is shown under the SXES spectra described by the relative energy Raman shift.⁷ The spectrum is largely composed of two parts; a Drude-like photoresponse near 0 eV due to the charge carriers and interband transitions observed at energies greater than 3 eV. A prominent peak is observed at ~ 5.5 eV (α peak) and a weak peak at ~ 6.8 eV (β peak) in addition to the broad γ band. It is reported that the α peak decreases with increasing La doping.⁷ The energy difference between α and β corresponds to the difference between nonbonding bands and the bonding band of the photoemission valence band. The SXES spectra are in good agreement with the optical conductivity spectrum, as shown in dashed lines

Figure 2 shows the SXES spectra of $La_{0.10}Sr_{0.90}TiO_3$, where the abscissa is the Raman shift that is the energy shift from the elastic scattering. The elastic scattering peak is located at 0 eV. The $Ti\ 3d \rightarrow Ti\ 2p$ fluorescence peaks shown by two vertical bars shift to the higher energy as the excitation energy increases. In $FeTiO_3$, it is reported that the structures appearing in the energy region between 11 and 4 eV can be attributed to the transition to nonbonding $3d^1L$ states and the split-off antibonding satellite is located at 14.5 eV.¹⁵ However, such a satellite is not observed in this figure.

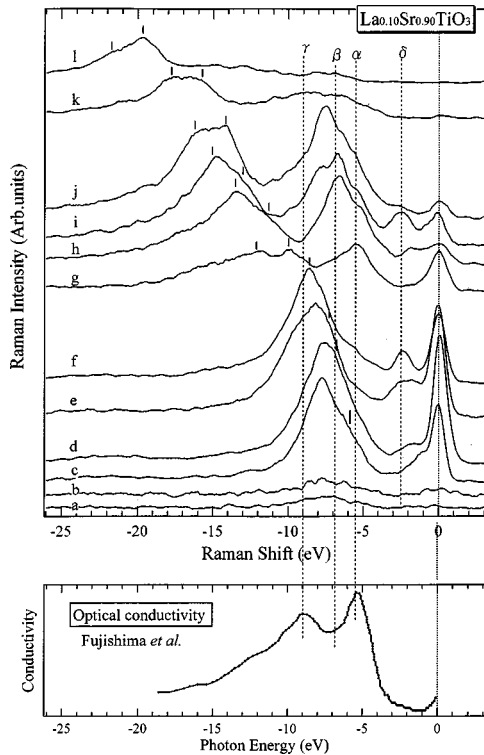


FIG. 2. The Ti $3d \rightarrow 2p$ SXES spectra of $\text{Sr}_{0.90}\text{La}_{0.10}\text{TiO}_3$ presented as the relative emission energy to the elastic scattering. For reference, the optical-conductivity spectrum taken from Ref. 7 is shown.

(α , β , γ). Thus, the α peak corresponds to the transition from nonbonding band to t_{2g} subband of Ti $3d$, and the β peak corresponds to the transition from bonding band to t_{2g} subband of Ti $3d$. In the SXES study on $3d^0$ compounds, the Raman scattering peak is observed at ~ 6.8 eV,^{12–14} which is attributed to a CT transition from occupied O $2p$ states to unoccupied Ti $3d$ states. However, Raman scattering at ~ 5.5 eV has not been found so far. These features reflect the CT-like character of the SXES spectra.^{12–16} The γ band at 9.2 eV corresponds to transitions from bonding band to e_g subband of Ti $3d$.

Figure 3 shows the SXES spectra as a function of doping at the e_g resonance of Ti in $\text{La}_x\text{Sr}_{1-x}\text{TiO}_3$. The intensity is normalized at the Ti $3d \rightarrow \text{Ti } 2p$ fluorescence peak. The δe_g peak is found in the band gap and its relative intensity increases with increasing La doping. We can determine the e_g resonance state by the Raman scattering. The Raman shift corresponds to the transition from the occupied t_{2g} subband to the unoccupied e_g subband, as shown in the inset of Fig. 3. The energy position of the $d-d$ transition represents the magnitude of the crystal-field splitting $10Dq$. This $10Dq$ refers to the crystal-field in the ground state without the core hole. The estimated value of $10Dq$ is ~ 2.3 eV. The $10Dq$ has been also obtained from the Ti $2p$ XAS. (Ref. 22) and is in good agreement with our results. However, there are large multiplet structures due to the existence of the core hole in Ti $2p$ XAS. Furthermore, the crystal field splitting should be different between with and without core hole. The energy position of the δe_g peak shows the small shift to the higher energy side as the La doping increases. This fact may be explained from the change of the lattice constant.^{6–8} It has

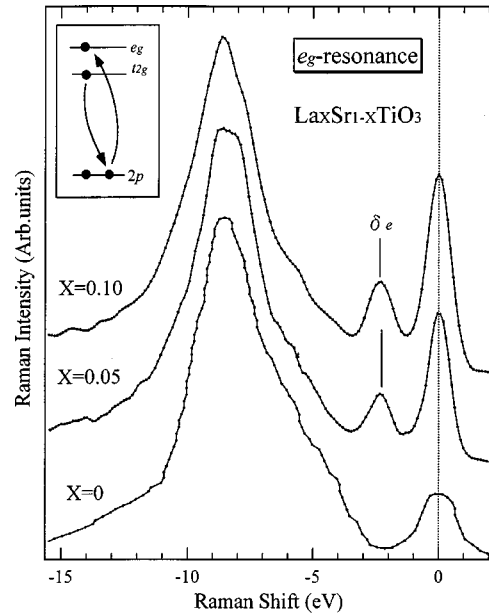


FIG. 3. Comparison of the e_g -resonance SXES spectra of $\text{La}_x\text{Sr}_{1-x}\text{TiO}_3$ ($x=0, 0.05, 0.10$). This e_g resonance spectrum obtained for $x=0.10$ is spectrum *f* in Fig. 1(b).

been reported that the lattice constant decreases, the crystal lattice is distorted by doping and the Ti-O-Ti bond angle decreases with increasing La doping (160° – 180° for $\text{La}_x\text{Sr}_{10-x}\text{TiO}_3$).^{3,4}

Figure 4 shows the SXES spectra as a function of doping at the t_{2g} resonance in $\text{La}_x\text{Sr}_{1-x}\text{TiO}_3$ ($x=0, 0.05, 0.10$). Comparing each spectrum, one notes that the intensity of the δt_{2g} peak in the band gap increases with increasing La doping. In the photoemission study of various compounds of $\text{La}_x\text{Sr}_{1-x}\text{TiO}_3$,¹¹ two features have been observed in the band gap below the E_F that are attributed to Ti $3d$ states. They are the coherent band at the E_F and the incoherent band at ~ 1.5 eV, as shown in the schematic diagram in the inset of Fig. 4. In the case of t_{2g} bands, there is typically no large

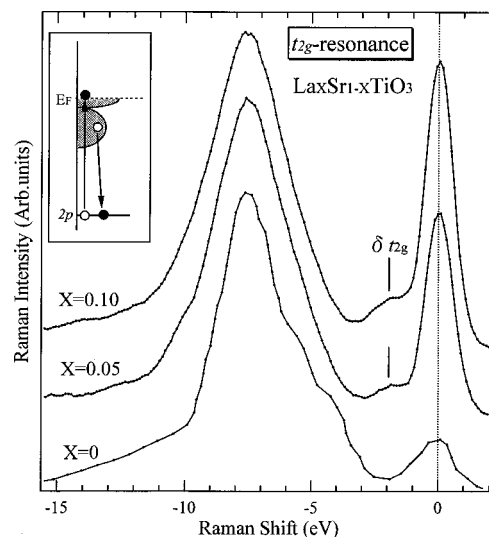


FIG. 4. Comparison of the t_{2g} -resonance SXES spectra of $\text{La}_x\text{Sr}_{1-x}\text{TiO}_3$ ($x=0, 0.05, 0.10$). This t_{2g} -resonance spectrum obtained for $x=0.10$ is spectrum *d* in Fig. 1(b).

band splitting so that the contribution to the Raman scattering is due to the electron correlation energy. From the previous information we suggest, the Raman scattering near ~ 2.2 eV corresponds to the transition between coherent and incoherent bands. The effective $U_{dd}/2$ has been estimated to be ~ 2.2 eV for $\text{La}_{0.10}\text{Sr}_{0.90}\text{TiO}_3$ from the analysis of Ti $2p$ core level photoemission spectra.²² This is in good agreement with the result presented in Fig. 4. The δt_{2g} peak does not shift much by doping. This fact indicates that the effective U_{dd} does not change much for $X < 0.5$. This is consistent with the results obtained from the effective mass and the electronic specific heat.^{8,9} Thus, the results of Figs. 3 and 4 indicate that the $M-I$ transition can not be attributed to electron correlation but to the change of the lattice constant and crystal distortion with the La doping with $x < 0.10$ of $\text{La}_x\text{Sr}_{1-x}\text{TiO}_3$.

The magnitude of this effective U_{dd} is in good agreement with the results of photoemission and inverse-photoemission studies.²²⁻²⁴ On the other hand, Kajuter *et al.*²⁴ indicates that the degree of correlation and disorder is larger at the

surface than in the bulk. This fact may explain the origin of the peak at ~ 1.5 eV below the E_F in the photoemission spectra. However, the present results suggest this peak exists as a bulk state, even though a surface state may also exist.

In conclusion, we have studied the soft x-ray scattering due to the charge transfer (CT) transition and compared the SXES spectra with the optical conductivity spectrum in the VUV region. The quantity of $10Dq$ decreases with La doping and is observed in the e_g resonance SXES spectra. The Raman scattering, which is attributed to the $d-d$ transition between the incoherent and the coherent bands, is directly observed in the t_{2g} -resonance SXES spectra of $\text{La}_x\text{Sr}_{1-x}\text{TiO}_3$ for $x < 0.10$. This Raman shift corresponds to the magnitude of the effective $U_{dd}/2$.

We would like to thank Dr. T. Yokoya for his useful discussions. We also acknowledge support from NSF Grant No. DMR-9017997, DOE-EPSCOR cluster research Grant No. DOE-LEQSF, and the Advanced Light Source by the Office of Basic Energy Science, U.S. Department of Energy Contract No. DE-AC03-76SF00098.

-
- ¹M. Cardona, Phys. Rev. **140**, A651 (1965).
²C. S. Koonce, M. L. Cohen, J. F. Shooley, W. R. Hosler, and E. R. Preiffer, Phys. Rev. **163**, 380 (1967).
³P. Calvani, M. Cappizi, F. Donato, S. Lupi, P. Maselli, and D. Peschiaroli, Phys. Rev. B **47**, 8917 (1993).
⁴C. Lee, J. Destry, and J. L. Brebner, Phys. Rev. B **11**, 2299 (1975).
⁵J. F. Shooley, W. R. Hosler, and M. L. Cohen, Phys. Rev. Lett. **12**, 474 (1964).
⁶Y. Tokura, Y. Taguchi, Y. Okada, T. Arima, K. Kumagai, and Y. Iye, Phys. Rev. Lett. **70**, 2126 (1993).
⁷Y. Fujishima, Y. Tokura, T. Arima, and S. Uchida, Phys. Rev. B **46**, 11 167 (1992).
⁸Y. Taguchi, Y. Tokura, T. Arima, and F. Inaba, Phys. Rev. B **48**, 511 (1993).
⁹Y. Fujishima, Y. Tokura, T. Arima, and S. Uchida, Physica C **185-189**, 1001 (1991).
¹⁰N. Shanthi and D. D. Sarma, Phys. Rev. B **57**, 2153 (1998).
¹¹A. Fujimori, I. Hase, H. Namatame, Y. Fujishima, Y. Tokura, H. Eisaki, S. Uchida, K. Takegawa, and F. M. F. de Groot, Phys. Rev. Lett. **69**, 1796 (1992); A. Fujimori, I. Hase, M. Nakamura, H. Namatame, Y. Fujishima, and Y. Tokura, Phys. Rev. B **46**, 9841 (1992).
¹²Y. Tezuka, S. Shin, A. Agui, M. Fujisawa, and T. Ishii, J. Phys. Soc. Jpn. **65**, 312 (1996).
¹³J. Jimenez-Mier, J. van Ek, D. L. Ederer, T. A. Callcott, J. J. Jia, J. Carlisle, L. Terminello, A. Asfaw, and R. C. Perera, Phys. Rev. B **59**, 2649 (1999).
¹⁴S. M. Butorin, J.-H. Guo, M. Magnuson, and J. Nordgren, Phys. Rev. B **55**, 4242 (1997).
¹⁵S. Shin, M. Fujisawa, H. Ishii, Y. Harada, M. Watanabe, M. M. Grush, T. A. Callcott, R. C. Perera, E. Z. Kurmaev, A. Moewes, R. Winarski, S. Stadler, and D. L. Ederer, J. Electron Spectrosc. Relat. Phenom. **92**, 197 (1998).
¹⁶S. M. Butorin, J.-H. Guo, M. Magnuson, P. Kuiper, and J. Nordgren, Phys. Rev. B **54**, 4405 (1996).
¹⁷S. M. Butorin, D. C. Mancini, J.-H. Guo, N. Wassdahl, J. Nordgren, M. Nakazawa, S. Tanaka, T. Uozumi, A. Kotani, Y. Ma, K. E. Myano, B. A. Karlin, and D. K. Shuh, Phys. Rev. Lett. **77**, 574 (1996).
¹⁸Y. Uehara, D. W. Lindle, T. A. Callcott, L. T. Terminello, F. J. Himpsel, D. L. Ederer, J. H. Underwood, E. M. Gullikson, and R. C. C. Perera, Appl. Phys. A: Mater. Sci. Process. **65**, 179 (1997).
¹⁹T. A. Callcott, K. L. Tsang, C. H. Zhang, D. L. Ederer, and E. T. Arakawa, Rev. Sci. Instrum. **57**, 2680 (1986).
²⁰F. M. F. de Groot, J. C. Fuggle, B. T. Thole, and G. A. Sawatzky, Phys. Rev. B **41**, 928 (1991).
²¹K. Okada and A. Kotani, J. Electron Spectrosc. Relat. Phenom. **1**, 71 (1995).
²²A. E. Bocquet, T. Mizokawa, K. Morikawa, A. Fujimori, S. R. Barman, K. Maiti, D. D. Sarma, Y. Tokura, and M. Onoda, Phys. Rev. B **53**, 1161 (1996).
²³D. D. Sarma, S. R. Barman, H. Kajuter, and G. Kotliar, Europhys. Lett. **36**, 307 (1996).
²⁴H. Kajuter, G. Kotliar, D. D. Sarma, and S. R. Barman, Int. J. Mod. Phys. B **11**, 3849 (1997).